Cross-Relaxation in Spin Systems*

N. Bloembergen, S. Shapiro, P. S. Pershan,† and J. O. Artman‡

Gordon McKay Laboratory, Harvard University, Cambridge, Massachusetts

(Received November 20, 1958)

The energy transfer between adjacent resonances in nuclear and electron spin systems is analyzed in terms of the overlap of line-shape functions. The procedure is an enlargement on the original proposal of Kronig and Bouwkamp, and consists of taking partial account of off-diagonal elements in the spin-spin interaction, which are omitted in Van Vleck's truncated Hamiltonian. If the frequency of these off-diagonal elements is sufficiently small, they give rise to an additional kind of spin-spin relaxation, observed by Gorter and co-workers. They are also responsible for cross-saturation effects in paramagnetic salts of the type observed by Townes and co-workers. A crucial experiment is described which can be explained by spin-spin interactions, but not by the assumption of a hot-phonon region. Implications of the cross-relaxation for the operation of solid state masers are discussed. Special consideration is given to magnetically dilute substances and inhomogeneously broadened lines. Paradoxically, the latter will usually still undergo a homogeneous steady-state saturation.

1. INTRODUCTION

SINCE Waller's fundamental paper[1] on spin relaxation and Gorter's early experiments,[2] much attention has been paid to the question of thermal equilibrium in magnetic spin systems. Casimir and du Pré[3] postulated the existence of such equilibrium within the spin system to explain the spin-lattice relaxation effects of Gorter and co-workers. Kronig[4] already realized that thermal equilibrium in the whole spin system would only be established if the dipolar interactions between different spins was sufficient to "bridge the gap" between the various spin levels of an individual ion.

With the advent of magnetic resonance techniques, the problem of magnetic relaxation gained new impetus. It was generally recognized that the populations of spin levels which are equally spaced readily attain the Boltzmann ratio, but the establishment of a Boltzmann distribution between spin levels with unequal spacing takes a much longer time. An early illustration[5,6] is the saturation in high magnetic field of one nuclear spin resonance without affecting the other species in the same crystal. The Li^7 and F^{19} spin systems in LiF are better isolated from one another in high fields than they are from the lattice. In magnetic fields below a hundred oersteds, however, they come more readily into equilibrium with one another. Use of this physical phenomenon has been made to reduce the relaxation time of a spin species by giving it the same

energy splitting as another species and thus bringing it into contact with another spin system with a shorter spin-lattice relaxation time.[6-8]

It is the purpose of this paper to analyze in some detail the transition region of nearly equally spaced levels. For equal spacing a Boltzmann distribution over the different spin levels is established in a time of the order of T_2. For unequal spacing they come into equilibrium with the lattice first with their respective relaxation times T_1. The Casimir-du Pré hypothesis is not valid in this case. In the intermediate region of approximately equal spacing, different parts of the spin system may come into internal equilibrium in an intermediate time, which we shall call the *cross-relaxation time* and designate by T_{21}. It will be shown that double flip-flops of neighboring spins in which the Zeeman energy is "nearly" conserved are responsible for this effect. The small balance of energy is taken up by the dipolar or internal energy of the spin system.

This raises the important problem of the equilibrium of the Zeeman (and quadrupolar or crystalline splitting) energy on the one hand and the dipolar interaction on the other, which is discussed in a very lucid manner by Abragam and Proctor.[6] These authors assume the existence of a mixing field H^* larger than the local dipolar field H_L. The energy splittings for $H < H^*$ are sufficiently small to allow for a rapid exchange of Zeeman and dipolar energy. Abragam and Proctor do not discuss the dynamics of spin interactions which would give a theoretical justification for the experimental observation of such mixing. One purpose of this paper is to provide a semiquantitative discussion of those processes which transform Zeeman and dipolar energy into each other.

Such processes can also give a quantitative explanation for the cross-saturation effects of adjacent electron

† National Science Foundation Predoctoral Fellow.
‡ Now at Applied Physics Laboratory, Johns Hopkins University, Silver Spring, Maryland.

[1] I. Waller, Z. Physik **79**, 370 (1932).
[2] C. J. Gorter, *Paramagnetic Relaxation* (Elsevier Publishing Company, Inc., Amsterdam, 1947).
[3] H. B. G. Casimir and F. K. du Pré, Physica **5**, 507 (1938).
[4] R. Kronig and C. J. Bouwkamp, Physica **5**, 521 (1938); **6**, 290 (1939).
[5] R. V. Pound and E. M. Purcell, Phys. Rev. **81**, 279 (1951).
[6] A. Abragam and W. G. Proctor, Phys. Rev. **109**, 1441 (1958).
[7] G. Feher and H. E. D. Scovil, Phys. Rev. **105**, 760 (1957).
[8] H. S. Gutowsky and D. E. Woessner, Phys. Rev. Letters **1**, 6 (1958).

spin resonances reported by Giordmaine and others.[9] Their suggestion of phonon heating over a certain frequency interval is ruled out by a cross-maser experiment described in this paper. The importance of cross-relaxation effects for band width characteristics and low-frequency limits of solid state masers is discussed. Preliminary discussions of these spin-spin interactions have been given.[10]

Finally, these processes are also responsible for the temperature-independent relaxation at intermediate frequencies discovered by de Vryer, Gorter, and others.[11,12] In a recent paper by Verstelle, Drewes, and Gorter[13] an interpretation of those results in terms of the same processes discussed here has been announced.

2. CROSS-RELAXATION TIME

Consider the spin Hamiltonian

$$\mathcal{3C} = \mathcal{3C}_m + \mathcal{3C}_{cr} + \mathcal{3C}_{int}, \tag{1}$$

$\mathcal{3C}_{cr}$ is the sum of the crystalline field couplings of the individual ions or the quadrupole couplings of the nuclei.

The Zeeman energy in the applied field is given by

$$\mathcal{3C}_m = -\sum_i \beta \mathbf{H} \cdot \mathbf{g}_i \cdot \mathbf{S}_i.$$

The interaction between the spins consists of dipolar, pseudodipolar, and exchange terms:

$$\mathcal{3C}_{int} = A + B + C + D + E + F, \tag{2}$$

$$A = \sum_{j>i} [A_{ij} + (g_i g_j \beta^2 r_{ij}^{-3} + B_{ij}) \times (1 - 3\cos^2\theta_{ij})] S_{zi} S_{zj}, \tag{2a}$$

$$B = \sum_{j>i} [\tfrac{1}{2} A_{ij} + (-\tfrac{1}{4})(g_i g_j \beta^2 r_{ij}^{-3} + B_{ij}) \times (1 - 3\cos^2\theta_{ij})] (S_{+i} S_{-j} + S_{-i} S_{+j}), \tag{2b}$$

$$C = \sum_{j>i} (-\tfrac{3}{2})(g_i g_j \beta^2 r_{ij}^{-3} + B_{ij}) \sin\theta_{ij} \times \cos\theta_{ij} e^{-i\phi_{ij}} (S_{+i} S_{zj} + S_{zi} S_{+j}), \tag{2c}$$

$$D = \sum_{j>i} (-\tfrac{3}{2})(g_i g_j \beta^2 r_{ij}^{-3} + B_{ij}) \sin\theta_{ij} \times \cos\theta_{ij} e^{+i\phi_{ij}} (S_{-i} S_{zj} + S_{zi} S_{-j}), \tag{2d}$$

$$E = \sum_{j>i} \tfrac{3}{4}(g_i g_j \beta^2 r_{ij}^{-3} + B_{ij}) \sin^2\theta_{ij} e^{-2i\phi_{ij}} S_{+i} S_{+j}, \tag{2e}$$

$$F = \sum_{j>i} \tfrac{3}{4}(g_i g_j \beta^2 r_{ij}^{-3} + B_{ij}) \sin^2\theta_{ij} e^{+2i\phi_{ij}} S_{-i} S_{-j}. \tag{2f}$$

θ_{ij} and ϕ_{ij} are the polar angles of the radius vector connecting ions i and j with respect to the z-axis.

Consider the simple case of a Kramers doublet with identical spins. Take the z-direction along H. The Zeeman splitting of each individual ion is

$$h\nu_{12} = +g\beta H.$$

It is assumed to be larger than the interaction with other ions. $\mathcal{3C}_{int}$ will be treated as a perturbation. The problem, which was already considered by Kronig and Bouwkamp,[4] is to determine the rate at which Zeeman energy and dipolar energy come into mutual equilibrium. Since total energy of the spin Hamiltonian remains conserved, the formulation can also be put in the form: What is the probability that a quantum $h\nu_{12}$ gets absorbed by a rearrangement in the dipolar lattice?

Consider repeated operation of the interaction Hamiltonian. Take products of the type $\cdots (S_{zk} S_{zl}) \times (S_{+m} S_{-n}) \cdots (S_{+i} S_{zj}) \cdots (S_{zp} S_{zq})(S_{+r} S_{-s})$. They turn the spin i in the external field and rearrange the dipolar lattice. It would be difficult to carry through such a high-order perturbation calculation.

A hybrid method between the perturbation calculation and the method of moments[14] is therefore used. Simple first order time-dependent perturbation theory is applied to the terms C and D (and possibly E and F). The repeated effect of the diagonal and semidiagonal terms A and B is absorbed in a line-shape function $g(\nu)$. The transition probability for the Zeeman energy $h\nu_{12}$ of a spin to be converted into dipolar energy is

$$w = (2T_{21})^{-1} = \hbar^{-2} |C|^2 N^{-1} g(\nu = 0). \tag{3}$$

The characteristic time for this conversion process is called T_{21} to indicate its intermediate position between T_1 and T_2. The shape function $g(\nu)$ has a symmetrical maximum around the frequency ν_{21}. Its second moment around this frequency is given by

$$h^2 \langle \Delta \nu^2 \rangle$$

$$= -\frac{\text{Tr}\{[(A+B)\sum_{j>i} S_{zi} S_{+j} - \sum_{j>i} S_{zi} S_{+j}(A+B)]^2\}}{\text{Tr}\{[\sum_{j>i} S_{zi} S_{+j}]^2\}}. \tag{4}$$

This moment has the same order of magnitude as, but is not identical with, the second moments of Van Vleck for transitions induced by an external radio-frequency field.

If the assumption of a Gaussian shape with the correct second moment (4) is made, the cross-relaxation probability becomes for $g_i = g_j$, $S_i = S_j$, $B_{ij} = 0$,

$$w = \frac{\hbar^{-2} \times \tfrac{3}{4} g^4 \beta^4 S(S+1) \sum_j r_{ij}^{-6} \sin^2\theta_{ij} \cos^2\theta_{ij}}{(2\pi)^{\frac{1}{2}} \langle \Delta\nu^2 \rangle^{\frac{1}{2}}} \times \exp\left\{\frac{-g^2\beta^2 H^2}{2h^2\langle\Delta\nu^2\rangle}\right\}. \tag{5}$$

The cross-relaxation time T_{21} increases very rapidly as the splitting of the energy levels of an individual ion becomes large compared to the spin-spin interaction. This is the reason why the processes with $\Delta m = \pm 2$, caused by the terms E and F are negligible. They would lead to an expression in which the exponent in

[9] Giordmaine, Alsop, Nash, and Townes, Phys. Rev. **109**, 302 (1958).

[10] Shapiro, Bloembergen, and Artman, Bull. Am. Phys. Soc. Ser. II, **3**, 317 (1958). Proceedings of the Symposium on Solid-State Masers, U. S. Army Signal Research and Development Laboratories, Fort Monmouth, New Jersey, June, 1958 (unpublished).

[11] F. W. de Vryer and C. J. Gorter, Physica **18**, 549 (1952).

[12] Smits, Derksen, Verstelle, and Gorter, Physica **22**, 773 (1956).

[13] Verstelle, Drewes, and Gorter, Physica **24**, 632 (1958).

[14] J. H. Van Vleck, Phys. Rev. **74**, 1168 (1948).

the Gaussian is 4 times larger than in (5). Hence their contribution is negligible.

When the splitting approaches zero $(H \to 0)$, the expressions (3) and (4) have to be modified. All terms of the dipolar interaction then become important. Truncation is not permissible. The second moment increases and also the matrix element in Eq. (3) is increased because the E and F terms also contribute. In the case that H is not much larger than the dipolar field, the formula of Kronig-Bouwkamp, who first considered the problem under discussion, should be valid:

$$w = [\langle \Delta\omega^2 \rangle_{\text{tot}}]^{\frac{1}{2}} \exp\{ -g^2\beta^2 H^2 / 2\hbar^2 \langle \Delta\omega^2 \rangle_{\text{tot}} \}.$$

It is seen that the cross-relaxation time T_{21} becomes identical with T_2 in the limit $H \to 0$. If, on the other hand, $T_{21} > T_1$, the Zeeman part and the spin-spin part come separately into equilibrium with the lattice. The hypothesis of Casimir and du Pré is not valid in that case. The interesting region is $T_1 > T_{21} > T_2$. In this domain the relaxation phenomena mentioned in the introduction occur.

A warning should be raised against too liberal use of the Gaussian shape, which is so convenient for computational purposes. The value of $g(0)$ may be larger by several orders of magnitude than the Gaussian would predict. Important situations, in which the tails are considerably enhanced, include the case of strong exchange interactions A_{ij} and the case of random paramagnetic dilution. Calculation of the fourth, and higher, moments of $g(\nu)$ shows the enhancement of the tail concomitant with a narrowing at the center.

Interesting new situations arise when three or more levels are considered or when more than one magnetic species is present. Some simple examples are shown in Fig. 1. In Figs. 1(a) and 1(b) the isolated atoms are assumed to have three energy levels. In case 1(a), two of them are closely spaced; in 1(b) one is approximately halfway between the others. They may correspond to a Ni^{++} ion, or nucleus with $I = 1$, in an axially symmetric
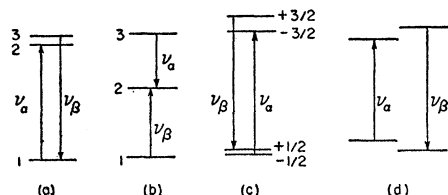

FIG. 1. Some representative situations of double transitions in which the energy is nearly conserved. The α and β transitions take place simultaneously on neighboring spins. (a) Three levels, two of which are closely spaced. Example: the Ni^{++} ion in an axial crystalline field with a small magnetic field. (b) Three levels, with one approximately halfway between the others. Example: Ni^{++} in intermediate field. (c) Two closely spaced pairs of levels. Example: Cr^{+++} or a nucleus with $I = \frac{3}{2}$ in an axial field, with a small magnetic field parallel to the axis. (d) Two Kramers doublets with nearly equal spacing. Example: two Cu^{++} ions with different nuclear spin orientations, or two nuclear spins $I = \frac{1}{2}$ with nearly equal γ in a relatively weak external field.

field with weak or intermediate external magnetic field, respectively. Case 1(c) corresponds to a case with S or $I = \frac{3}{2}$. Case 1(d) corresponds, e.g., to two species $I_\alpha = I_\beta = \frac{1}{2}$, with slightly different gyromagnetic ratios.

The dipolar interaction between the ions may induce transitions in which the sum of Zeeman and crystalline field energies is nearly conserved. These transitions are indicated by the arrows. It should be noted that the two arrows in each case belong to different ions. The balance of energy is again taken up by the spin-spin energy.

The probability per unit time for the process that ion i increases its energy by an amount $h\nu_\alpha$ and ion j decreases its energy by $h\nu_\beta$, the balance of energy $h(\nu_\beta - \nu_\alpha)$ being taken up by the spin-spin interaction of the whole array of dipoles, is then given by

$$w_{ij} = \hbar^{-2} | (E_i, E_j | \mathcal{3C}_{ij} | E_i + h\nu_\alpha, E_j - h\nu_\beta) |^2 g_{\alpha\beta}(\nu = 0), \quad (6a)$$

where $\mathcal{3C}_{ij}$ is the interaction between ions i and j.

If m_s is a good quantum number in case 1(d) and the gyromagnetic ratio has the same sign for the two species, the matrix element corresponds to the $\Delta m_s^\alpha = -\Delta m_s^\beta = \pm 1$ transition from the interaction B in Eq. (2) and its square is given by

$$| \mathcal{3C}_{ij} |^2 = \frac{1}{16} (I_\alpha - m_\alpha)(I_\alpha + m_\alpha + 1)(I_\beta + m_\beta)$$
$$\times (I_\beta - m_\beta + 1) g_i^2 g_j^2 \beta^4 (1 - 3 \cos^2\theta_{ij})^2 r_{ij}^{-6}. \quad (7a)$$

If, however, the gyromagnetic ratios g_i and g_j have opposite sign, the transition which nearly conserves energy has $\Delta m = \pm 2$ and is determined by the E or F term in Eq. (2). This is also true for cases 1(a), (b), and (c), if a magnetic field parallel to the axis of the crystalline field is applied. In the case of Cr^{+++} ion in a small parallel field one has, for example, the transition $m_z^\alpha = \frac{3}{2} \to \frac{1}{2}$ and $m_z^\beta = -\frac{1}{2} \to -\frac{3}{2}$.

$$| \mathcal{3C}_{ij} |^2 = (81/16) g_{||}^4 \beta^4 r_{ij}^{-6} \sin^4\theta_{ij}. \quad (7b)$$

The shape function $g_{\alpha\beta}(\nu)$ is calculated by the moment method. The total second moment is

$$h^2 \nu_{\alpha\beta}^2 = -\text{Tr}\{ [\mathcal{3C}(\sum \mathcal{3C}_{ij}) - (\sum \mathcal{3C}_{ij})\mathcal{3C}]^2 \} /$$
$$\text{Tr}\{ [\sum \mathcal{3C}_{ij}]^2 \}. \quad (8a)$$

The total Hamiltonian $\mathcal{3C}$ has to be truncated in a manner appropriate to the particular problem at hand.[15] If m_s is a good quantum number, this truncation is straightforward. The line shape has a maximum at the frequency $\nu_\alpha - \nu_\beta$; $g_{\alpha\beta}(\nu = 0)$ will be appreciable, if $h(\nu_\alpha - \nu_\beta)/g\beta$ is not much larger than the local fields.

It is instructive to obtain an estimate of $g_{\alpha\beta}(\nu = 0)$ in terms of the observed magnetic resonance lines $g_\alpha(\nu)$ and $g_\beta(\nu)$. The second moments of these shape functions are determined by the expression which results if $\sum \mathcal{3C}_{ij}$ in Eq. (8a) is replaced by S_x. The rigorous

[15] Ishiguro, Kambe, and Usui, Physica 17, 310 (1951).

expression (6a) is replaced by

$$w_{ij} = \hbar^{-2} |\mathfrak{IC}_{ij}|^2 \int \int g_\alpha(\nu')g_\beta(\nu'')\delta(\nu'-\nu'')d\nu'd\nu''. \quad (6b)$$

If a Gaussian shape is assumed for $g_\alpha(\nu)$ and $g_\beta(\nu)$ with second moments $(\Delta\nu_\alpha)^2$ and $(\Delta\nu_\beta)^2$, respectively, the integrations in (6b) which represent the overlap between the two resonances can be carried out explicitly. The result is

$$w_{ij} = (2\pi)^{-\frac{1}{2}}\hbar^{-2}|\mathfrak{IC}_{ij}|^2[(\Delta\nu_\alpha)^2+(\Delta\nu_\beta)^2]^{-\frac{1}{2}}$$
$$\times \exp\{-(\nu_\alpha-\nu_\beta)^2/2[(\Delta\nu_\alpha)^2+(\Delta\nu_\beta)^2]\}. \quad (8b)$$

This expression is not rigorous and should be used with extreme caution. Equations (6a) and (8a) should be preferred, but $g_{\alpha\beta}(\nu=0)$ is of course not determined by (8a) alone. All higher moments are necessary in principle. The assumption of a Gaussian with the second moment given by Eq. (8a) may still lead to large errors in the tail.

A cross relaxation time T_{21} can be defined by the relation

$$(2T_{21}{}^\alpha)^{-1} = \sum_j w_{ij}p_j{}^\beta. \quad (9)$$

This derivation has physical validity and significance in the range $T_1 > T_{21} > T_2$. The right-hand side represents the probability that spin i will absorb a quantum $h\nu_\alpha$, while an arbitray spin j emits a quantum $h\nu_\beta$; $p_j{}^\beta$ represents the probability for a spin j to be in the upper state of a ν_β transition.

It is noteworthy that there is no need for very closely spaced levels. Figure 1(b) shows that the only requirement is that some spacings are nearly equal. If closely spaced levels exist, as in Fig. 1(a), no matrix element between them is required. The Zeeman energy of the $m = \pm 1$ levels of Ni^{++} in an axial crystalline field with parallel magnetic field can come into Boltzmann equilibrium with the spin-spin energy via the indicated process.

3. CONSERVATION OF ANGULAR MOMENTUM

In the experiments of Abragam and Proctor, as in other adiabatic (de−) magnetization experiments, the angular momentum of the spin system is not conserved. Nor is it in the processes of Kronig and Bouwkamp or in the $\Delta m = \pm 2$ processes considered in the preceding section. For those who are familiar with the magneto-mechanical experiments of Einstein-de Haas and Barnett,[16] the answer is obvious that the balance of angular momentum is transferred to the rigid lattice and appears as a rotation of the whole crystal. Since the question of angular momentum has been raised on more than one occasion, a brief general proof will be given that the transition probabilities which have been derived are correct, even though the question of angular momentum has been ignored.

The coordinate Φ giving the azimuthal orientation

---

[16] C. J. Gorter and B. Kahn, Physica 7, 753 (1940).

of the rigid crystal with respect to a fixed coordinate system is introduced explicitly. The angle ϕ_{ij} measures the azimuthal orientation of the spin pair i and j with respect to a coordinate system attached to the crystal. The z axes of the two systems of reference coincide. Replace ϕ_{ij} in Eqs. (2) by $\phi_{ij}+\Phi$. The angular momentum associated with the rotation of the crystal is represented by the operator $(\hbar/i)(\partial/\partial\Phi)$. The total angular momentum around the z-axis is given by

$$J_z = \sum_j S_{zj} + \frac{\hbar}{i}\frac{\partial}{\partial\Phi}.$$

It can readily be verified that this operator commutes with the Hamiltonian (1):

$$[J_z, \mathfrak{IC}] = 0.$$

The spin angular momentum $\sum_j S_{zj}$ alone does not commute with the dipolar interaction, but total angular momentum is indeed conserved. If the spin system undergoes a transition $\Delta m = +2$, the angular momentum of the crystal changes by $-2\hbar$. The change in rotational energy associated with this change in rotation is negligible because of the very large mass of the crystal. The value of the square of the matrix element $|\mathfrak{IC}_{ij}|^2$ is not changed by the explicit introduction of Φ and the free rotational wave functions for the crystalline lattice.

4. CROSS-RELAXATION RATE PROCESSES

The rate equations governing the populations of the various spin levels should now be modified to take account of the cross-relaxation of Sec. 2. They will be written down explicitly for the cases of Figs. 1(a) and 1(d). Extension to other, more complicated, situations is straightforward.

Case 1(a).—Let n_1, n_2, and n_3 represent the populations in the three levels. The equilibrium values at the lattice temperature are $n_1{}^0$, $n_2{}^0$ and $n_3{}^0$. The energy difference $h\nu_{21}=E_2-E_1$ is so much larger than the dipolar interaction that no cross-relaxation has to be considered to the ground level E_1. The splitting $h\nu_{32}=E_3 -E_2$ is only slightly—say, two to ten times—larger than the dipolar width. Cross-relaxation has to be considered due to the overlap of the ν_{31} and ν_{21} resonances, although their maxima are experimentally well resolved. The populations n_2 and n_3 can now change also by the cross-relaxation processes. Note that the population n_1 is not affected.

$$(\partial n_2/\partial t)_{\text{cross rel}}$$
$$= -(\partial n_3/\partial t)_{\text{cross rel}} = w[n_3-n_2-(n_3-n_2)_{\text{ad}}]$$
$$+ N^{-1}\sum_j w_{ij}[(n_3n_1-n_2n_1)-(n_3n_1-n_2n_1)_{\text{ad}}].$$

Here w corresponds to the Kronig-Bouwkamp process described by Eq. (3). The w_{ij}, which are given by Eqs. (6) or (8), correspond to the double flips indicated in Fig. 1(a) and their inverses,

The equilibrium value of the population to which the cross-relaxation mechanism tends asymptotically is not given by the Boltzmann distribution at the lattice temperature. The equilibrium value is determined by the requirement that the expectation value of the total spin Hamiltonian (1) changes by the work done during the variation of the external field. The processes are adiabatic in the sense that no heat is transferred to or from the lattice.

In the limit of high temperatures, $kT \gg h\nu_{31}$, the dipolar interaction energy can be defined separately from the Zeeman and crystalline field energy. Let T_l be the lattice temperature, $T_z{}^i$ the initial "Zeeman temperature" defined by $h\nu_{32}k^{-1} \ln(n_2/n_3)$, $T_s{}^i$ the initial dipolar temperature, defined by $E_{\mathrm{dip}} = \langle \mathcal{3C}_{\mathrm{int}}{}^2 \rangle / kT_s$, and T_{ad} the final temperature after the spin system has come into internal equilibrium adiabatically. This equilibrium is to be understood in a partial sense, as only those levels participate between which cross-relaxation processes are important.

The usual relations between populations and spin temperature exist.

$$(n_3 - n_2)_{\mathrm{ad}} = \tfrac{1}{2}(N - n_1)(h\nu_{32})(1/kT_{\mathrm{ad}}). \quad (10)$$

The adiabatic condition can be written

$$-\int M dH_0 = \tfrac{1}{4}(N-n_1)(h\nu_{32})^2[(1/kT_z{}^i) - (1/kT_{\mathrm{ad}})]$$
$$+ \mathrm{Tr}(\mathcal{3C}_{\mathrm{int}}{}^2)[(1/kT_s{}^i) - (1/kT_{\mathrm{ad}})]. \quad (11)$$

In the high-temperature limit, n_1/N may be replaced by $\tfrac{1}{3}$.

Introduce next the spin-lattice relaxation mechanism and radio-frequency fields at ν_{13} and ν_{23}. The complete rate equations then become, in the same notation as used for three-level masers,[17]

$$\frac{dn_3}{dt} = W_{31}(n_1 - n_3) + W_{32}(n_2 - n_3)$$
$$+ w_{13}\left(n_1 - n_3 - \tfrac{1}{3}N\frac{h\nu_{31}}{kT_l}\right)$$
$$+ w_{23}\left(n_2 - n_3 - \tfrac{1}{3}N\frac{h\nu_{32}}{kT_l}\right)$$
$$+ (w + \tfrac{1}{3}\sum_j w_{ij})\left[n_2 - n_3 - \tfrac{1}{3}N\frac{h\nu_{32}}{kT_{\mathrm{ad}}}\right], \quad (12)$$

$$\frac{dn_2}{dt} = W_{32}(n_3 - n_2) + w_{23}\left(n_3 - n_2 + \tfrac{1}{3}N\frac{h\nu_{32}}{kT_l}\right)$$
$$+ w_{12}\left[n_1 - n_2 - \tfrac{1}{3}N\frac{h\nu_{21}}{kT_l}\right]$$
$$- (w + \tfrac{1}{3}\sum_j w_{ij})\left[n_2 - n_3 - \tfrac{1}{3}N\frac{h\nu_{32}}{kT_{\mathrm{ad}}}\right].$$

This set of equations should, strictly speaking, be supplemented with an equation describing the direct relaxation of the dipolar energy to the lattice. It will turn out that in many applications the details of this process and the exact value of T_{ad} are of no importance.

Case 1(d).—Consider a lattice with N_α ions with two energy levels separated by $h\nu_\alpha$ and N_β ions with two energy levels separated by $h\nu_\beta$, $\nu_\alpha - \nu_\beta \ll \nu_\alpha$. The cross-relaxation processes contribute the following term to the rate equations for the difference in population of the two α-levels and the two β-levels:

$$(\partial \Delta n_\alpha / \partial t)_{\mathrm{cross}} = -(\partial \Delta n_\beta / \partial t)_{\mathrm{cross}}$$
$$= -2N_\beta^{-1}\sum_{j=1}^{N_\beta} w_{ij}[(n_\alpha{}^+ n_\beta{}^- - n_\alpha{}^- n_\beta{}^+)$$
$$- (n_\alpha{}^+ n_\beta{}^- - n_\alpha{}^- n_\beta{}^+)_{\mathrm{ad}}]. \quad (13)$$

In the high-temperature approximation, $kT \gg h\nu_\beta$, Eq. (13) can be put in the form

$$(\partial \Delta n_\alpha / \partial t)_{\mathrm{cross}} = -(1/T_{21}{}^\alpha)\{\Delta n_\alpha - (\Delta n_\alpha)_{\mathrm{ad}}\}$$
$$+ (1/T_{21}{}^\beta)\{\Delta n_\beta - (\Delta n_\beta)_{\mathrm{ad}}\},$$

where $(1/T_{21}{}^\alpha) = (N_\beta/N_\alpha)(1/T_{21}{}^\beta)$, and $p_j{}^\beta = \tfrac{1}{2}$ is substituted in Eq. (9).

The complete rate equations in the presence of spin-lattice relaxation[18] and an applied radio-frequency field at the frequency ν_α become

$$\frac{d(\Delta n_\alpha)}{dt} = -2W_\alpha \Delta n_\alpha - \frac{1}{T_1{}^\alpha}\left(\Delta n_\alpha - \tfrac{1}{2}N_\alpha \frac{h\nu_\alpha}{kT_l}\right)$$
$$- \frac{1}{T_{21}{}^\alpha}\left(\Delta n_\alpha - \tfrac{1}{2}N_\alpha \frac{h\nu_\alpha}{kT_{\mathrm{ad}}}\right)$$
$$+ \frac{1}{T_{21}{}^\beta}\left(\Delta n_\beta - \tfrac{1}{2}N_\beta \frac{h\nu_\beta}{kT_{\mathrm{ad}}}\right),$$

$$\frac{d(\Delta n_\beta)}{dt} = -\frac{1}{T_1{}^\beta}\left(\Delta n_\beta - \tfrac{1}{2}N_\beta \frac{h\nu_\beta}{kT_l}\right)$$
$$+ \frac{1}{T_{21}{}^\alpha}\left(\Delta n_\alpha - \tfrac{1}{2}N_\alpha \frac{h\nu_\alpha}{kT_{\mathrm{ad}}}\right)$$
$$- \frac{1}{T_{21}{}^\beta}\left(\Delta n_\beta - \tfrac{1}{2}N_\beta \frac{h\nu_\beta}{kT_{\mathrm{ad}}}\right). \quad (14)$$

These rate equations will now be used to interpret a number of relaxation experiments. Although in practice the energy level diagrams are often considerably more complicated than those shown in Fig. 1, Eqs. (12) and (14) for cases 1(a) and 1(d) contain all the essential features. The construction of rate equations for cases

---

[17] N. Bloembergen, Phys. Rev. 104, 324 (1956).

[18] To avoid further nonessential complications, spin-lattice processes in which the two species participate in a coupled fashion, such as those considered by I. Solomon [Phys. Rev. 99, 559 (1955)], are ignored.

1(b) and 1(c) and for more intricate situations should be straightforward.

5. INTERMEDIATE RELAXATION IN LEIDEN EXPERIMENTS

Paramagnetic dispersion and absorption have been found at intermediate frequencies $(1/T_2) \gg \omega \gg (1/T_1)$. This dispersion is independent of the lattice temperature and may show maxima as a function of an applied dc magnetic field.[11-13] A simple theoretical model, patterned after the treatment of spin-lattice relaxation by Kronig and Gorter,[19] for this new type of relaxation is presented here. A similar explanation has also been announced by the Leiden group.[13]

Let $\Delta H \exp(i\omega t)$ be a small periodic magnetic field in an arbitrary direction. In general the energy levels will shift by $(\partial E/\partial H)\Delta H \exp(i\omega t)$. There is a periodic variation of the populations $\Delta n \exp(i\omega t)$ and a concomitant variation in the magnetic moment. Let us take model 1(a), which applies to the Ni^{++} ion. Substitute the periodic variation on the left-hand sides of Eqs. (12). If $w \gg w_{12}, w_{13}, w_{23}$, the spin-lattice relaxation terms are negligible. The applied field is not at a resonance frequency and hence $W_{31}=W_{32}=0$. The periodic variation of the populations in this region is described simply by

$$i\omega(n_3-n_2) = 2(w+\tfrac{1}{3}\sum w_{ij})[n_2-n_3-(n_2-n_3)_{ad}]. \quad (15)$$

The solution is

$$n_3-n_2 = (n_3-n_2)_{ad}(1+i\omega T_{21})^{-1}. \quad (16)$$

Here $T_{21}=\tfrac{1}{2}(w+\tfrac{1}{3}\sum w_{ij})^{-1}$ is determined by Eqs. (3) and (6). The population n_1 remains constant.

The susceptibility must now be calculated. The magnetization is given by

$$M = \tfrac{1}{2}(n_3-n_2)(M_{33}-M_{22}) + \tfrac{1}{2}(n_3+n_2)(M_{33}+M_{22})$$
$$+ n_1 M_{11} + \text{contributions from off-diagonal}$$
$$\text{elements of the magnetic moment operator.} \quad (17)$$

Only the first term on the right-hand side is frequency-dependent in the range of interest. Its contribution goes to zero as $\omega \gg T_{21}^{-1}$.

The adiabatic value $(n_3-n_2)_{ad}$ is calculated from the condition that the work done by the variation of the external field is equal to the sum of the changes in Zeeman energy and interaction energy, with the restriction that only effects arising from a variation in n_3-n_2 should be taken into account.

With the relations

$$M_{33}-M_{22} = \frac{\partial(h\nu_{32})}{\partial H}, \quad n_3-n_2 = \tfrac{1}{3}N\frac{h\nu_{32}}{kT},$$

$$(n_3-n_2)_{ad} = \frac{\partial(n_3-n_2)}{\partial H_{ad}}\Delta H \exp(i\omega t), \quad (18)$$

[19] See reference 2, Chap. 4.

Eq. (11) can be put in the differential form

$$\tfrac{1}{6}N\frac{(h\nu_{32})}{kT}\frac{\partial h\nu_{32}}{\partial H} = \left(\frac{\partial}{\partial H}\right)_{ad}\left[\tfrac{1}{2}\times\tfrac{1}{3}N\frac{(h\nu_{32})^2}{kT} + \frac{\langle \mathcal{H}_{int}^2\rangle}{kT}\right].$$

This can be further transformed into

$$\left(\frac{\partial}{\partial H}\right)_{ad}(n_3-n_2) = \frac{\langle \mathcal{H}_{int}^2\rangle}{\tfrac{1}{6}N(h\nu_{32})^2+\langle \mathcal{H}_{int}^2\rangle}\frac{N}{3}\frac{h}{kT}\frac{\partial\nu_{32}}{\partial H}. \quad (19)$$

Combining Eqs. (16), (17), (18) and (19), one finds for the part of the susceptibility which undergoes the intermediate relaxation

$$\chi'-i\chi'' = \frac{\langle \mathcal{H}_{int}^2\rangle \times \tfrac{1}{6}Nh^2/kT}{\tfrac{1}{6}N(h\nu_{32})^2+\langle \mathcal{H}_{int}^2\rangle}\left(\frac{\partial\nu_{32}}{\partial H}\right)^2\frac{1}{1+i\omega T_{21}}. \quad (20)$$

The behavior of χ' as a function of frequency is shown schematically in Fig. 2. The solid curve is for the larger separation of the two levels, the dotted curve has a smaller value of ν_{32}. There is the usual spin-lattice relaxation. For $\omega > T_1^{-1}$ the susceptibility drops to its "adiabatic value." Then the intermediate relaxation of part of this adiabatic susceptibility occurs at $\omega \approx T_{21}^{-1}$. The dispersion is temperature-independent and is a very sensitive function of the separation of the levels because of T_{21}.

Experimentally, the susceptibility is usually plotted at constant frequency *versus* applied dc field. There may easily occur a maximum in this plot, because for certain values of the external field some pairs of levels of the chromium, manganese, and ferric salts may become nearly equidistant. This will make T_{21} about equal to ω^{-1}. For the Cu^{++} ion, which has a Kramers doublet, such a maximum of $\chi'(\omega)$ vs H should not occur, in agreement with observation. With the
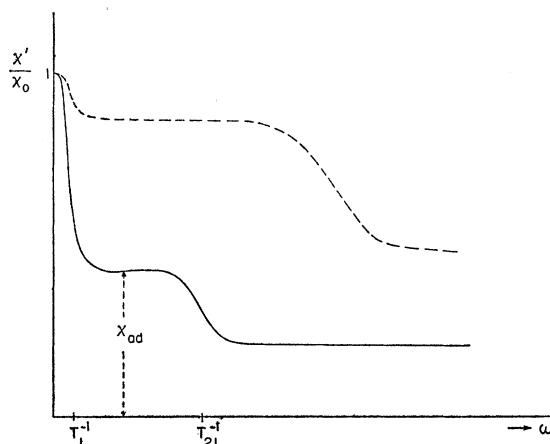

Fig. 2. Qualitative behavior of the real part of the susceptibility in a dilute paramagnetic salt as a function of frequency, showing spin-lattice relaxation and cross-relaxation. The solid curve is for the case where the difference in spacing between the energy levels is slightly larger than the dipolar field; the dotted curve is for the opposite case. There may be several regions of cross-relaxation in systems with many spin levels.

multiple levels of the Cr^{+++}, Mn^{++}, and Fe^{+++} ions, and the presence of several nonequivalent sites in the unit cell, the occurrence of several intermediate relaxation regions is assured. The theory for such multilevel situations can be patterned after the simple case 1(a) given here. The algebra will become quite involved. Since in most experiments polycrystalline powders have been used, an average over all orientations of H with respect to the crystalline fields should be taken. This makes a detailed comparison of published relaxation curves with theory too cumbersome.

Relaxation experiments should be carried out in dilute single crystals. Contributions of individual pairs of levels to the susceptibility may be separated. The experimental data should be plotted *versus* frequency at constant H, because then the energy levels of the ion remain fixed.

In concentrated paramagnetic salts the dipolar interaction may indeed be sufficient to connect all levels with a reasonably short T_{21}, close to the value T_2, so that the Casimir-du Pré hypothesis has validity. In very high fields or for very large crystalline fields, the validity of the hypothesis should break down even for the concentrated salts. The lumping of the crystalline field with the dipolar field in the expressions for the adiabatic susceptibility should be avoided. It is permissible only in polycrystalline powders of concentrated magnetic salts.

6. THERMAL CONTACT IN NUCLEAR SPIN SYSTEMS

The classic experiments on nuclear spin temperature and thermal contact between spin systems have been carried out in lithium fluoride.[6] It was found that the Li and F nuclear spins are well isolated from each other in external fields larger than a few hundred oersteds. They then come separately into equilibrium with the lattice in times of the order of several minutes. However, they come into equilibrium with each other in 6 seconds in a field of 75 oersteds and in less than 0.1 second in a field of 40 oersteds.

The appropriate model of spin levels is case 1(d). Although Li^7 has $I=\frac{3}{2}$ and four equally spaced levels rather than just two, Eqs. (14) can still be used. These two coupled linear equations of the first order will in general give two relaxation times λ^{-1} determined by

$$\{(1/T_1{}^\alpha)+(1/T_{21}{}^\alpha)-\lambda\}\{(1/T_1{}^\beta)+(1/T_{21}{}^\beta)-\lambda\}$$
$$-(1/T_{21}{}^\alpha T_{21}{}^\beta)=0. \quad (21)$$

A linear combination of two exponentials adapted to the initial conditions describes the complete decay to the lattice temperature.

The interest here is in the situation that $T_{21}{}^{\alpha,\beta}\ll T_1{}^{\alpha,\beta}$. The two spin systems come into adiabatic equilibrium at T_{ad} with a characteristic time $[(T_{21}{}^\alpha)^{-1}+(T_{21}{}^\beta)^{-1}]^{-1}$ $=N_\beta T_{21}{}^\alpha/(N_\alpha+N_\beta)$. The experiment is carried out in a

short time interval, so that subsequent decay to T^l cannot take place.

In agreement with the experimental results, the heat contact should set in rather suddenly below a critical value of the external magnetic field. Equation (8b) indicates that two Gaussian resonances separated by twice their full width at half maximum have a cross-relaxation time of $T_{21}\approx10^{+4}T_2$. This shows that two well-resolved resonances may indeed mix in a time shorter than T_1. If they are separated by three times their full width, the mixing time is $T_{21}\approx10^7T_2$, which will usually be longer than T_1. Substitution of the second-moment values for Li^7 and F^{19} into (8b), with use of Eqs. (7a) and (9), gives $T_{21}=10^{12}$ sec at $H_0=75$ oersteds. This is many orders of magnitude longer than the observed value of 6 seconds. The Gaussian function is of course extremely sensitive to small variations in the effective second moment. It is tempting to invert the procedure and use the observed cross-relaxation time as a measure of the overlap and hence as an exceedingly sensitive tool to measure the line shape far in the wing.

In the case of LiF, for example, the wings will have some bumps. It should be noted that the Zeeman energy is more nearly conserved when two Li^7 nuclei flip $\Delta m_{Li}=2$, for each $\Delta m=-1$ of the F^{19} nuclei. The square of the matrix element $|\mathcal{3C}_{ij}|^2$ in Eq. (6a) for these processes is smaller by a factor $(\langle\Delta\nu^2\rangle_{Li}/\nu_{Li}{}^2)$ $\times[(\nu_F-2\nu_{Li})/\nu_F]^2\approx3\times10^{-4}$ for $H_0=75$ oersteds, but this is more than offset by the enormous increase in the Gaussian function, which now has $(\nu_F-2\nu_{Li})^2$ instead of $(\nu_F-\nu_{Li})^2$ in the exponent. The factor in square brackets is included to take account of the partial cancellation of terms in the second-order perturbation calculation, as will be discussed in more detail in Sec. 7. In terms of the moment method one may say that the truncation of $\mathcal{3C}$ should not exclude terms $I_{+Li}I_{zj}$. Inclusion of such terms gives rise to small bumps in $g(\nu)$ near the frequency $\nu_F-2\nu_{Li}$. If the approximation of the overlap integral (6b) is used, one finds the value of the cross-relaxation time is 3 seconds, which is in excellent agreement with the experimental value of 6 seconds. At $H_0=40$ oersteds, the cross-relaxation time should be 0.06 second, again in agreement with observation.

Experiments by one of us (P.S.P.) are under way to determine accurately the shape of the overlap as a function of the external field. Cross-relaxation time measurements may also be useful to detect quadrupole background broadening. Similar experiments are also being carried out by various other workers.[20,21]

It can be concluded that all observations on energy transfer between nuclear spin systems are consistent with the theory of spin-spin interaction presented in

[20] R. T. Schumacher, Phys. Rev. **112**, 837 (1958).
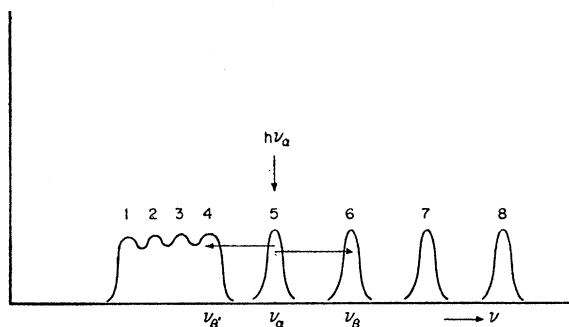[21] M. J. Weber and E. L. Hahn, Bull. Am. Phys. Soc. Ser. II, **3**, 329 (1958).

FIG. 3. A reproduction of the resonances in $Cu(NH_4)_2(SO_4)_2$ $\cdot 6H_2O$ observed by GANT, taken from Fig. 1 of reference 9. Resonance 5 is saturated. The arrows indicate a process of multiple spin flips by which the energy is spread through the structure and cross-saturation occurs. Each arrow represents the simultaneous flip-flop of two spins. The change in Zeeman energy is equal to the length of the arrow. Zeeman energy is conserved for two arrows of equal and opposite length. Four spins are involved in such a process.

this paper. In particular, the discussion of Abragam and Proctor is entirely justified. Their condition that a spin process be adiabatic in the thermodynamic sense can now be made more quantitative:

$$\frac{1}{H_0}\frac{dH_0}{dt} \ll \frac{1}{T_{21}}.$$

This condition is usually not fulfilled if $\gamma H_0 > 5\langle\Delta\omega^2\rangle^{\frac{1}{2}}$. For such high external fields, however, the difference in magnetization in an adiabatic change of H_0 and the constant magnetization in a rapidly changing H_0 is less than 5%.

7. CROSS-SATURATION EFFECTS IN PARAMAGNETIC SALTS

A series of stimulating experiments on paramagnetic resonance saturation and relaxation at liquid helium temperatures in magnetically dilute gadolinium magnesium nitrate, chromium potassium cyanide, and copper ammonium Tutton salt have been reported by Giordmaine, Alsop, Nash, and Townes.[22] Since the most detailed experimental results were obtained on $Cu(NH_4)_2(SO_4)_2\cdot 6H_2O$, attention will be focused on this salt. There are two nonequivalent Cu^{++} ions in the unit cell and the paramagnetic resonance spectrum consists of sets of four lines, corresponding to the four orientations of the copper nuclear spin. A reproduction of these eight lines as observed by GANT[22] is shown in Fig. 3. The spacing of the hyperfine components in one set was about 100 oersteds. The other set, which had more closely spaced lines, was separated by about 100 oersteds from one hyperfine component in the first set. The full width at half-maximum of each component was 20 oersteds. This width is caused mainly by interactions with proton spins. The dipolar

[22] See reference 9. This paper will henceforth be referred to as GANT.

interactions between the copper ions in the diluted salt would give only 3 oersteds. The relaxation time $T_1 = 20$ sec.

The most striking observations were cross-saturation effects, i.e., on steady-state saturation of one of the eight lines, some or all of the others would also show saturation. Furthermore, if one resonance was inverted or saturated by adiabatic rapid passage, it was observed to recover very rapidly in intensity with a characteristic time of $10^{-3} - 10^{-4}$ sec $\ll T_1$.

An interpretation of these results is proposed in terms of the spin-spin interactions described by Eqs. (14). This interpretation is very different from the hot-phonon theory proposed by GANT.

It has already been shown in the case of nuclear resonance that the combination of spin-lattice and of cross-relaxation gives rise to two characteristic times given by Eq. (21). In the case that $T_{21} \ll T_1$, these two times are just T_{21} and T_1. The short time, 10^{-4} sec, may be identified with T_{21}. In this time the intensity of a resonance is shared with adjacent resonances and since there are a total of eight resonances, the intensity of a saturated transition results in a time T_{21} to within 15% of its equilibrium value.

The cross-saturation is described by the steady-state solution of Eqs. (14). Note that the ions α and β may be two copper ions in different crystallographic positions or similar Cu^{++} ions with different nuclear orientations. The α Cu^{++} ion is saturated by a resonance field at ν_α with an induced transition probability W_α.

If terms of the order of $h(\nu_\alpha - \nu_\beta)/kT_l$ and $h(\nu_\alpha - \nu_\beta)/kT_{ad}$ are neglected compared to unity, the steady-state solution of the relative intensity of the α transition may be written in the form

$$\frac{\chi_\alpha''}{\chi_{\alpha,0}''} = 1 \bigg/ \left[1 + 2W_\alpha\left(\frac{1}{T_1^\alpha} + \frac{1}{T_1^\beta}\frac{T_{21}^\beta/T_{21}^\alpha}{1 + T_{21}^\beta/T_1^\beta}\right)^{-1}\right]. \quad (22)$$

If $T_{21}^\beta = T_{21}^\alpha \ll T_1$, it is seen that the α resonance is saturated as if it had an effective relaxation time $\{(1/T_1^\alpha) + (1/T_1^\beta)\}^{-1}$.

This relaxation is at the root of the apparent discrepancy between the determination of T_1 from the steady-state saturation experiments by Eschenfelder[23] and the Leiden results[24] on spin-lattice relaxation in dilute chromium salt. In the latter case, one measures the rates $(1/T_1^\alpha)$, $(1/T_1^\beta)$, and $(1/T_1^\gamma)$ for the various spin levels, or averages of these quantities over all orientations in the unit cell and crystallites in the powder. In the steady-state saturation, one measures the much faster rate $\sum_j (1/T_1^j)$, summed over all resonances j which, through cross-relaxation, are also saturated.

[23] A. H. Eschenfelder and R. T. Weidner, Phys. Rev. 92, 869 (1953).
[24] Van der Marel, van den Broek, and Gorter, Physica 23, 361 (1957).

The intensity of the β-resonance showing the cross-saturation is simply

$$(\chi_\beta''/\chi_{\beta,0}'')-1=[(\chi_\alpha''/\chi_{\alpha,0}'')-1]$$
$$\times(1+N_\beta T_{21}{}^\alpha/N_\alpha T_1{}^\beta)^{-1}. \quad (23)$$

For $N_\alpha=N_\beta$ and $T_{21}{}^\alpha \ll T_1{}^\beta$, the α and β resonances are saturated to the same degree. The β resonance remains unsaturated only when $T_{21}{}^\alpha \geq T_1{}^\beta$.

Is it reasonable to expect cross-relaxation times between 10^{-1} and 10^{-4} sec for the resonances of GANT shown in Fig. 3? A superficial application of Eq. (8b) seems to indicate that the spin-spin cross-relaxation time is longer than T_1. For a separation of the resonances by 100 oersteds and a calculated dipolar width of less than 3 oersteds, Eq. (8b) would give $T_{21} \approx e^{+300}T_2$. This result is an erroneous application of the theory.

The shape of a line in a crystal with random magnetic dilution is not a Gaussian with Van Vleck's value of the second moment. The experimental line shape is narrower in the center and much more intense in the wings as first shown by Abrahams and Kittel.[25] If the magnetic dilution is f, and Z the number of nearest neighbors, the chance for an ion to have a neighboring magnetic ion is Zf. The second-moment contribution of a magnetic nearest neighbor is roughly Z^{-1} times the second moment in the concentrated salt. If $Zf\ll1$, the situations in which more than one neighboring ion is magnetic may be ignored. An expression replacing Eq. (8) which should approximate the overlap of wings in dilute magnetic materials would be

$$T_{21} \approx (Zf)^{-1}(\Delta\nu_\alpha{}^2)_{\text{conc}}{}^{-\frac{1}{2}} \exp\left\{\frac{Z(\nu_\alpha-\nu_\beta)^2}{2[\langle\Delta\nu_\alpha{}^2\rangle_{\text{conc}}+\langle\Delta\nu_\beta{}^2\rangle_{\text{conc}}]}\right\},$$

with $f=10^{-2}$, $Z=8$, $\langle\Delta\nu_\alpha{}^2\rangle_{\text{conc}}=\langle\Delta\nu_\beta{}^2\rangle_{\text{conc}}=200$ Mc/sec, $\nu_\alpha-\nu_\beta=280$ Mc/sec, this yields $T_{21}\approx10^3 T_2{}^{\text{conc}}$.

This admittedly very qualitative argument gives order-of-magnitude agreement with the experimental cross-relaxation times. It should be realized that the shape of far wings is not well known and the argument here is that a reasonable shape of the wing can give the required overlap.

A more potent mechanism in the case of eight copper resonances is provided by the observation that quadruple spin flips can exactly conserve the Zeeman energy.

A process of simultaneous double flip-flops is indicated in Fig. 3. Two ions make a downward transition at the frequency ν_α, while ions at frequencies ν_β and $\nu_{\beta'}$ go up. Consider in general four spins α, α', β, β' with $S=\frac{1}{2}$. The effect of nuclear spins and local fields of other spins in the crystal is lumped with the Zeeman energy. The α, α' spins are initially upward, the β, β' spins downward. If all spins are reversed, energy is conserved:

$$\nu_\alpha+\nu_{\alpha'}-\nu_\beta-\nu_{\beta'}=0.$$

[25] C. Kittel and E. Abrahams, Phys. Rev. 90, 238 (1953).

The matrix element of the dipolar interaction which connects the initial and final "Zeeman-state" derives its most important contribution from a double application of the operators of type B [Eq. (2b)] because of the assumed inequalities of the type

$$|A| < |\nu_\alpha-\nu_\beta| < \nu_\alpha.$$

The matrix element is consequently

$$B_{\alpha\beta}B_{\alpha'\beta'}[h(\nu_\beta-\nu_\alpha)+A_{\alpha\alpha'}+A_{\beta\beta'}+A_{\alpha\beta'}+A_{\beta\alpha'}]^{-1}$$
$$+B_{\alpha'\beta'}B_{\alpha\beta}[h(\nu_{\beta'}-\nu_{\alpha'})+A_{\alpha\alpha'}+A_{\beta\beta'}+A_{\alpha\beta'}+A_{\beta\alpha'}]^{-1}$$
$$+B_{\alpha\beta'}B_{\beta\alpha'}[h(\nu_\alpha-\nu_{\beta'})+A_{\alpha\alpha'}+A_{\beta\beta'}+A_{\alpha\beta}+A_{\alpha'\beta'}]^{-1}$$
$$+B_{\alpha'\beta}B_{\alpha\beta'}[h(\nu_{\alpha'}-\nu_\beta)+A_{\alpha\alpha'}+A_{\beta\beta'}+A_{\alpha\beta}+A_{\alpha'\beta'}]^{-1}.$$

The matrix element vanishes if the dipolar interactions of the type A given by Eq. (2a) are ignored. Then the energy denominators of the first term and the second term, in which the two flip-flops occur in reverse order, would have opposite sign. Similarly, the third and fourth terms would cancel each other. If the $\alpha\beta$ pair and $\alpha'\beta'$ pair are very far apart, the dipolar terms $A_{\alpha\alpha'}$, $A_{\beta\beta'}$, $A_{\alpha\beta'}$, and $A_{\beta\alpha'}$ will be small. They are calculated from Eq. (2a) by allowing a change in quantum number of one constituent, $\Delta S_i=\pm1$. It is reasonable that the probability for a simultaneous act of two pairs vanishes, if there is no physical interaction between the pairs.

The probability per unit time for the quadruple spin flip is then obtained in the usual way by squaring the matrix element and integrating over a narrow frequency range around the maximum.

The order of magnitude can be estimated by considering the case that $\alpha\beta$ are a pair of nearest neighbors, and so is $a'\beta'$. The distance between the two pairs corresponds to the average distance in the diluted salt. The probability for this initial situation is $(Zf)^2$. It is not necessary to introduce additional factors of $\frac{1}{8}$ to specify $\alpha\beta$, $\alpha'\beta'$ among the eight possible states. The equal spacing between components appears to make double flip-flops possible in most configurations. The probability then becomes

$$w \approx \hbar^{-2}|A|_{\text{dilute}}{}^2 g_{\max}(\nu)(Zf)^2[|B|_{\text{neighbor}}{}^2/h^2(\nu_\alpha-\nu_\beta)^2]^2,$$

or

$$T_{21} \approx (T_2)_{\text{dilute}}(Zf)^{-2}|B|_{\text{neighbor}}{}^{-4} h^4(\nu_\alpha-\nu_\beta)^4.$$

With $Zf=10^{-1}$ and $B_{\text{neighbor}}/h(\nu_\alpha-\nu_\beta)\approx\frac{1}{3}$, one finds $T_{21}\approx10^4 T_2$ in excellent agreement with the observations.

Worded in a different way, the true line shape of each resonance is not Gaussian, but has small bumps which fall just under an adjacent resonance. These side bumps are of a similar nature to those shown by Van Vleck.[14] He omitted these in the truncation of the Hamiltonian for the purpose of calculating the second moment. Here we should not cut off the terms in $S_{+\alpha}S_{-\beta}$ between different ions although we do omit other terms in the dipolar interaction. The bumps in the wing are extremely important, because the interest

is in processes which may be more than a million times slower than T_2. The exact values of the cross-relaxation times will be sensitive to the exact positioning of the lines, but values of T_{21} ranging between $10^3 T_2$ and $10^6 T_2$ can hardly be avoided. It is believed that this is the most effective mechanism in the copper salt. It explains the rapid transfer of energy to the wing components if the central resonances are saturated and can also account for the asymmetry and partial cross-saturation if a line in the wing is saturated.

The possibility of spin-spin processes had been ruled out by GANT on the basis of the observation that a strong microwave field applied at a frequency between the two resonances does not produce saturation. The assumption hidden in this argument is that the energy would have to be transported from resonance ν_α to ν_β via the small fraction of spins resonating in intermediate fields. The essence of the spin-spin processes is, however, that a jump from resonance $\nu_\alpha \rightarrow \nu_\beta$ can be made, the balance of energy being taken up by a large number of transitions within the resonances ν_α and ν_β, or, even better, as explained in the preceding paragraph, the jump from resonance $\nu_\alpha \rightarrow \nu_\beta$ is accompanied by a simultaneous jump $\nu_\gamma \rightarrow \nu_\delta$, with $\nu_\alpha + \nu_\gamma \approx \nu_\beta + \nu_\delta$.

From a similar viewpoint it may be said that the radio-frequency field, off resonance, still produces transitions at the frequency ν_α, while the balance of energy is again taken up by multiple spin rearrangements. The transition probability for such an induced transition is reduced by a factor $g(\nu - \nu_\alpha)/g_{\max}(0)$. In order to produce saturation of the α-resonance the microwave intensity should be stepped up by a factor 10^6 or more, if applied far away from resonance. Sufficient power cannot be fed into the spin system in the far wings to combat spin-lattice relaxation in the center of the resonance.

It is therefore concluded that spin-spin interactions offer a possible explanation for the cross-saturation effects of GANT. Further discussion of and comparison with their hot-phonon theory will be postponed until the final section.

8. INHOMOGENEOUS BROADENING AND HOMOGENEOUS SATURATION

In sufficiently diluted magnetic substances the line width is usually determined by local variations of nuclear spin arrangements or a distribution of crystalline field parameters. Inasmuch as the dipolar interactions between the ions contribute only a small fraction of the observed second moment, the line is said to have an inhomogeneous broadening.

This type of inhomogeneity should be carefully distinguished from that produced by a gradient in the external fields or by the use of a polycrystalline anisotropic material. In the latter case spins in different parts of the crystal or in different crystallites have different resonant frequencies. Different spin popula-

tions in different parts of the resonant curve can only come into equilibrium by spin diffusion in space.[26] This is a very slow process and inhomogeneous saturation—"eating a hole"—occurs readily.[27]

In the former microscopic type of inhomogeneous broadening, adjacent spins will have quite different resonant frequencies. The situation is then more a problem of spin diffusion in the frequency domain rather than in space. The problem can be considered as the cross-effect between two resonances α and β both of which have the same continuous distribution. A qualitative solution can readily be given. Assume that the resonances with a dipolar second moment $\langle \Delta \nu^2 \rangle$ are distributed uniformly over a frequency interval $(1/T_2^*)$. Take a frequency ν_α in this distribution. The probability to make a cross-transition to ν_β is of the order of T_2^{-1} if $\nu_\alpha + \frac{1}{2}T_2^{-1} < \nu_\beta < \nu_\alpha + \frac{1}{2}T_2^{-1}$ and is essentially zero outside this interval. The probability that the ν_β of an adjacent spin is indeed in the required interval is T_2^*/T_2. The most probable time to cover a frequency interval T_2^{-1} is therefore $T_2(T_2/T_2^*)$. To diffuse across the whole distribution $(T_2/T_2^*)^2$ steps have to be taken. The time required for an absorbed quantum to diffuse through the inhomogeneous resonance[28] would be T_2^4/T_2^{*3}.

This random step model ignores the existence of quadruple and higher-order spin flips of the type indicated in Fig. 4. Under certain conditions this mechanism may be faster than the diffusion process. If the time $(T_{21})_{\text{multiple}}$ or $T_2^4/(T_2^*)^3$ is shorter than T_1, the inhomogeneous structure will show homogeneous saturation in the steady state. If by a short pulse a small fraction near the center of the structure has been saturated or inverted, this "hole" will be distributed evenly over the entire structure in a time $T_2^4/(T_2^*)^3$, and subsequent return to the lattice temperature will occur in a time T_1. Such effects, depicted in Fig. 4,
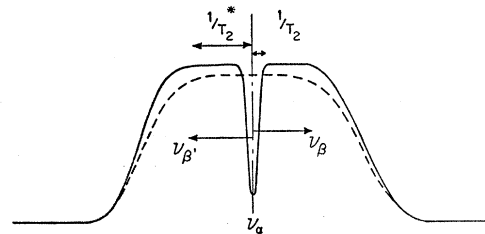

FIG. 4. Inhomogeneous line, saturated by a short radio-frequency pulse at ν_α. The line recovers to the dotted curve in a time $T_{21} \approx T_2^4/T_2^{*3}$ by simultaneous flip-flops indicated by arrows. Further recovery to equilibrium takes a time T_1.

[26] N. Bloembergen, Physica 15, 286 (1949).
[27] Bloembergen, Purcell, and Pound, Phys. Rev. 73, 679 (1948).
[28] A. M. Portis, Phys. Rev. 104, 584 (1956), has considered spin-diffusion in the frequency domain in more detail. His method would give a characteristic time T_2^6/T_2^{*5}. The multiple spin flips will always give an answer shorter than this time, and should then always be taken into account. We are indebted to Professor Portis for correspondence on this point.

have been observed by Bowers and Mims[29] in nickel fluosilicate.

These effects are apparently the same in nature as those which occur between the eight resonances in the copper Tutton salt. The only difference is that there the eight resonances are discrete, while in an inhomogeneous structure a continuous distribution occurs. With the possible exception of extremely dilute magnetic substances (less than $1:10^4$), it appears that homogeneous saturation should be the rule rather than the the exception. In the steady-state saturation factor $\gamma^2 H_1^2 T_1 T_2$, the value of T_2 should usually be taken as T_2^*, the inverse of the observed total width. An alternative way of stating this fact is to say that Eq. (22) for the saturation factor has to be used with T_2/T_2^* resonances in parallel.

Finally, the general case of two inhomogeneously broadened structures will be discussed briefly.

Consider two rectangular inhomogeneous resonances A and B. It is tempting to argue that if the center of A is saturated the energy will diffuse to the edge of the A distribution. Then the Gaussian overlap of the true resonance shapes which are represented by the dotted lines will take it to the edge of B whence it will diffuse further. Due to the narrow width of the true resonances, the middle step is very slow. A much faster way can again be devised—e.g., by a sixfold spin flip. The three arrows in Fig. 5 show the three simultaneous flip-flops which conserve energy and transfer one spin from the A to the B resonance.

No attempt will be made here to develop a mathematical theory of random walk with multiple steps. The distribution of splittings will in general not have a rectangular shape. For a Gaussian shape, the random walk theory for an harmonically bound particle may be applied,[30] but multiple steps will again complicate the picture further.

9. A CRUCIAL EXPERIMENT: THE CROSS-MASER EFFECT. FURTHER IMPLICATIONS FOR MASER OPERATION

It has been shown that spin-spin interactions can account satisfactorily for all observations made by GANT. They have used the model of a "hot-phonon" region to explain the results. How can a choice be made between these two different interpretations?
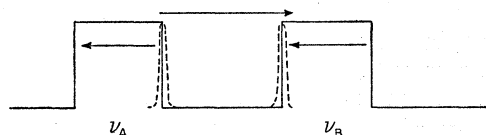
FIG. 5. Two rectangular inhomogeneous line structures. The energy contact is not through the wings of the true line shapes, but through multiple spin flip-flops, indicated by the arrows.

[29] K. D. Bowers and W. B. Mims, Bull. Am. Phys. Soc. Ser. II, 3, 325 (1958).
[30] Noise and Stochastic Processes, edited by N. Wax (Dover Publications, New York, 1954), c.f. p. 305.
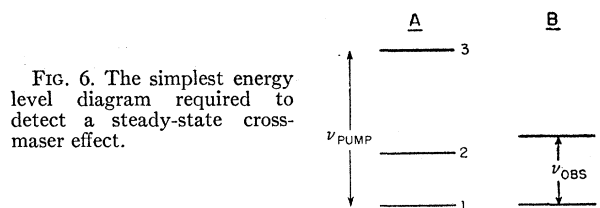
FIG. 6. The simplest energy level diagram required to detect a steady-state cross-maser effect.

In the first place, the experiments on LiF and other nuclear spin systems at room temperature show that spin-spin processes are capable of producing cross-saturation. A "hot-phonon" region is out of the question in this case, as the lattice vibrations are a good thermal reservoir at room temperature. The existence of similar spin-spin processes must therefore be admitted in electron-spin systems. Since they alone can give a satisfactory explanation of the observations, there is no need to invoke a second mechanism.

An attempt has been made to show the existence of cross-saturation effects in dilute $K_3Cr(CN)_6$ at 77°K. At this temperature the spin-lattice relaxation should take place predominantly by Raman processes. Phonons of all frequencies participate and constitute a thermal reservoir without limited heating. Unfortunately, T_1 at 77°K is too short so that no saturation could be obtained.

There is, however, another positive criterion. There is one thing a spin-spin contact can do which hot phonons cannot do. Spin-spin interactions can produce not only cross-saturation, but even cross-maser effects. They can, in other words, establish a contact at negative temperatures.[31] This is already contained in Eq. (23). χ_β'' can be negative, if $\chi_\alpha'' < 0$, and the last factor is sufficiently close to or larger than unity. This will be true when $N_\alpha \approx N_\beta$, $T_{21}^\alpha \ll T_1^\beta$. The system of energy levels of an harmonic oscillator has no upper bound and such a system cannot attain negative temperature.[32] The α-system at a negative temperature could therefore heat the phonons at most to an infinite positive temperature. The hot-phonon mechanism could never give $\chi_b'' < 0$.

A critical experiment would require a salt containing one ion, species α, with three spin levels and another, species β, with two spin levels. The first ion should be made emissive at the frequency ν_α by three-level maser pumping. The $\chi''(\nu_\beta)$ of the well-resolved but nearby resonance ν_β should then be observed, as indicated in Fig. 6.

Unfortunately such a paramagnetic substance is not readily available, and the actual experiment was performed on two nonequivalent Cr atoms in $K_3(0.995 \text{ Co})(0.005 \text{ Cr})(CN)_6$. The spin levels are sketched in Fig. 7. The magnetic field was applied in the ab plane which contains the z-axes of the crystalline fields for both ions. The magnetic field was near 1080 oersteds

[31] N. F. Ramsey, Phys. Rev. 103, 20 (1956).
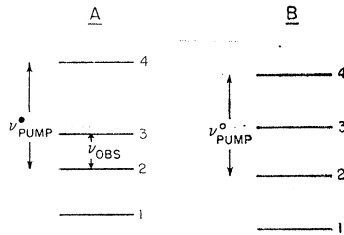[32] J. H. Van Vleck, Suppl. Nuovo cimento 6, 1081 (1957).

FIG. 7. Energy levels of two nonequivalent Cr^{+++} spins. The transitions indicated correspond to the experimental points in Figs. 8 and 9. It is also possible to observe the ν_{32} transition of B, while saturating either A or B.

and made angles of 4°30' and 16°30' with the principal crystal field axes of the two ions. The transition frequencies ν_{32} fell in the L-band, the pump frequencies ν_{24} in the X-band. The maser cavity was tunable at X-band frequency by a sliding coupling diaphragm. A $\lambda_g/4$ section on both sides provided good electrical connection with the fixed guide. Data were taken at 4.2°K on a small crystal to get reliable values for χ''.

The ordinary self-saturation curves of the ions at X-band, i.e., $\chi_A''(\nu_{24})$ vs $H_{rf, A}^2(\nu_{24})$ and $\chi_B''(\nu_{24})$ vs $H_{rf, B}^2(\nu_{24})$, are shown in Fig. 8. The two ions saturate at different power levels because of the different matrix elements in the two different orientations. These data will be needed in the subsequent analysis.

In Fig. 9 the L-band susceptibility $\chi_A''(\nu_{32})$ of ion A is plotted as a function of power saturation at X-band of ion A (closed points) or ion B (open points). The magnetic field was held fixed at 1087 oersteds. The X-band tuning was changed. The two X-band resonances are 210 Mc/sec apart, the L-band resonances are just resolved at 50 Mc/sec. Note that the "cross-maser" effect is stronger than the "self-maser" effect.

This last situation is no longer true if the L-band resonances are separated further. Figure 10 shows the data, when $H_0 = 1080$ oersteds, but makes angles of 10°30' and 22°30' with the axes at the two Cr ions in the unit cell. The L-band resonances are now separated by 150 Mc/sec, the X-band resonances by 250 Mc/sec.

Finally, the L-band resonances of ion B have been observed under the same conditions as the data in Fig. 9, except that the magnitude of H_0 was changed by 15 oersteds. These data are represented by curves 1
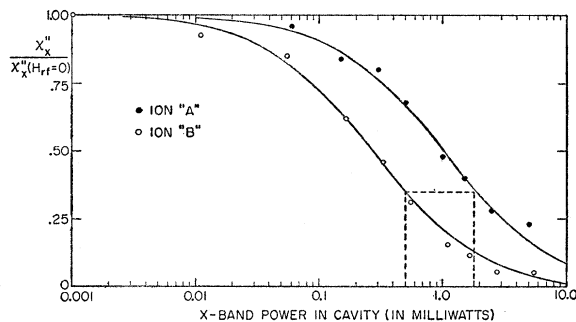

FIG. 8. Self-saturation curves for the X-band transitions of ions A and B. Magnitude and orientation of the field are the same as in Figs. 9 and 11. The solid curves obey the theoretical expression $(1+cH_{rf}^2)^{-1}$.

and 4 in Fig. 11. The data of Fig. 9 are repeated for comparison. For ion B the self-maser effect is stronger than the cross-maser effect.

An interpretation of these data in terms of the hot-phonon theory is now attempted. Cross-maser action may result from cross-saturation between the two X-band resonances. The location of the bottom levels, as illustrated in Fig. 7, is such that none of the frequencies ν_{12}, ν_{13}, ν_{14} lies in the vicinity of the observed transitions. Their existence will be ignored in the following discussion.

At most, ion A can be saturated to the same extent as ion B when $H_B^2(\nu_{24})$ is applied. With the aid of the dotted lines in Fig. 8 the value $H_A^2(\nu_{24})$ is obtained, which would give the same saturation of $\chi_A''(\nu_{24})$. With the self-maser curve in Fig. 9 one can plot the corresponding maser effect given by the crosses and the dotted line. This computed curve practically coincides
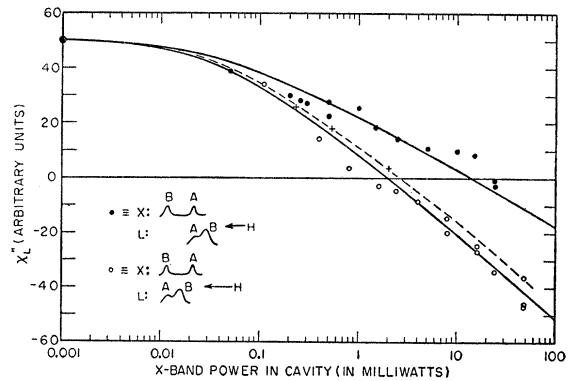

FIG. 9. Self- and cross-maser effects of ion A. Full circles: $\chi_A''(\nu_{32})$ vs $H_A^2(\nu_{24})$. Open circles: $\chi_A''(\nu_{32})$ vs $H_B^2(\nu_{24})$. The magnetic field of magnitude 1087 oersteds makes angles of 4°30' and 16°30' with the crystalline field axes of the two ions. The crosses are points calculated on the basis of maximum phonon interaction at X-band and zero phonon interaction at L-band. The inserts represent the observed line profiles.

with the observed curve for the cross-maser effect. If L-band hot-phonon interaction were admitted, the dotted curve would be pushed towards the axis $\chi'' \rightarrow 0$. Then a discrepancy would result. The data of Fig. 9 could be explained by a complete phonon heat interchange between the X-band resonances (210 Mc/sec apart) and no phonon contact between the L-band resonances (50 Mc/sec apart). This explanation is unlikely, but possible.

The data of Fig. 10 show that the cross-maser effect becomes much smaller when the X-band resonances are separated by 250 Mc/sec rather than 210 Mc/sec. This would indicate a drastic decrease from 100% phonon contact at 210 Mc/sec separation to less than 30% contact at 250 Mc/sec.

The situation becomes impossible, however, if we try to explain also the self- and cross-maser effect on ion B, given by curves 1 and 4 in Fig. 11. Again the

construction with Fig. 8 is used. If there really is
100% phonon contact at 210 Mc/sec separation between
the X-band resonances, the cross effect on ion B
should have been much larger and χ'' of curve 1 should
have gone through zero at 3 milliwatts instead of 70
milliwatts. The conclusion is that the hot-phonon
theory cannot account for all observations of Figs. 8–11.

If the contact by spin-spin interactions is adopted, a
quite natural explanation results. Since the X-band
resonances are far apart, cross-saturation at X-band
is assumed to be small. The contact between the L-band
resonances can be estimated from the pair of curves
3 and 4 in Fig. 11 to be about 80%, which is reasonable.
If we take the pair of curves 1 and 2, for both of which
the X-band resonance of ion A is saturated, one gets
70% for this contact. It is possible that a small cross-
saturation at X-band is still present. Presumably this
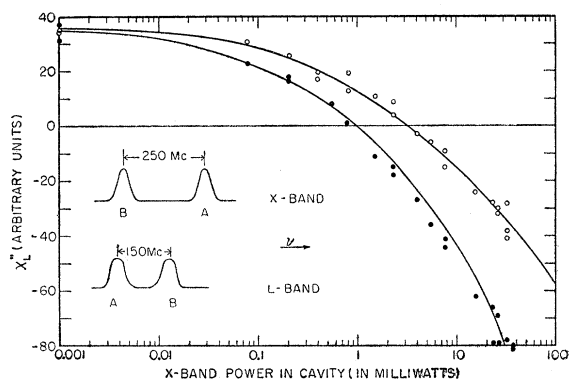would then also be caused by spin-spin interactions.

FIG. 10. Self- and cross-maser effects of ion A. Full circles:
$\chi_A''(\nu_{32})$ vs $H_A^2(\nu_{24})$. Open circles: $\chi_A''(\nu_{32})$ vs $H_B^2(\nu_{24})$. The
magnetic field of magnitude 1080 oersteds makes angles of 10°30′
and 22°30′ with the crystalline field axes of the two ions. The
inserts represent the line profiles as a function of frequency.
Due to different values of $\partial\nu/\partial H_0$ for different resonances the
observed profiles vs H_0 have different widths.

The smaller cross-saturation in Fig. 10 also follows
readily from the much reduced overlap of the L-band
resonances. It is also clear why the absolute value of
the self-maser effect is increased. The L-band A
resonance does not have to "drag along" the L-band
B resonance to the same extent as in Fig. 9.

Spin-spin interactions alone can account for all
observations of Figs. 8–11. Hot phonons do not have to
be invoked at all.

The entire resonance at the frequency ν_{32} appears to be
inverted. The bandwidth over which a paramagnetic
salt in a three-level maser is emissive is equal to the
entire width of the observed resonance curve. Even if
it has a so-called inhomogeneous line width, the maser
effect will be homogeneous. This statement is contrary
to one made by GANT. It is of great importance for
the operation of a three-level maser. It is, within wide
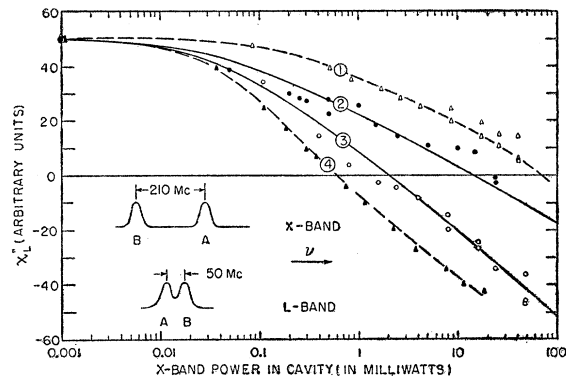limits, immaterial whether the paramagnetic resonance

FIG. 11. Self- and cross-maser effects of ions A and B. △ Curve 1:
$\chi_B''(\nu_{32})$ vs $H_A^2(\nu_{24})$, at $H_0=1072$ oersteds. ● Curve 2: $\chi_A''(\nu_{32})$
vs $H_A^2(\nu_{24})$, at $H_0=1087$ oersteds. ○ Curve 3: $\chi_A''(\nu_{32})$ vs $H_B^2(\nu_{24})$,
at $H_0=1087$ oersteds. ▲ Curve 4: $\chi_B''(\nu_{32})$ vs $H_B^2(\nu_{24})$, at H_0
$=1072$ oersteds. Curves 2 and 3 are the same as in Fig. 9. The
inserts represent the line profiles as a function of frequency.
Due to different values of $\partial\nu/\partial H_0$ for different transitions, the
observed profiles vs H_0 shown in Fig. 9 have a different appearance.
The angles between H_0 and the principal axes of the two non-
equivalent ions are 4°30′ and 16°30′ for all four curves.

is broadened homogeneously or inhomogeneously on
a microscopic scale. The saturation will occur homo-
geneously over the entire pumping frequency resonance
and the salt will amplify over the entire maser frequency
resonance.

This statement is in agreement with observations on
the band width of a traveling-wave maser,[33] and the
observed gain-bandwidth product of various cavity-
type masers. It has been pointed out previously[34] by
one of us (N.B.) that three-level maser action is
incompatible with a dominant interaction with hot
phonons. The steady-state condition would then be
one of three hot-phonon regions and three saturated
resonances.

The lower frequency limit ν_{23} of a three-level maser
is set by the overlap of the resonances ν_{13} and ν_{12}.
The steady-state solution of Eq. (12) in the limit of
heavy pumping $W_{31}\to\infty$, $n_1-n_3\to0$ becomes

$$n_3-n_2=\frac{1}{3}\frac{hN}{kT}\frac{-(w_{32}+w+\frac{1}{3}\sum_j w_{ij})\nu_{32}+w_{21}\nu_{21}}{w_{23}+w_{21}+2(w+\frac{1}{3}\sum_j w_{ij})}.$$

The condition for maser action becomes now

$$w_{21}\nu_{21}\gg(w_{32}+w+\tfrac{1}{3}\textstyle\sum_j w_{ij})\nu_{32}.$$

This cannot be fulfilled if the cross-relaxation time
becomes much shorter than T_1:

$$w+\tfrac{1}{3}\textstyle\sum_j w_{ij}\gg w_{21},\ w_{32}.$$

This will be a reason for maser failure at low frequencies
and with more concentrated paramagnetic salts. The

[33] Degrasse, Schulz-Dubois, and Scovil, Bell System Tech.
J. 38, 305 (1959).
[34] N. Bloembergen, Phys. Rev. 109, 2209 (1958).

overlap is of course a very sensitive function of ν_{32} and concentration.

The experimental results of Strandberg et al.[35] are also reinterpreted. It is clear from the spacing of energy levels in Fig. 3. of this reference that the cross-saturation effect can account very well for the operation of the S-band maser without invoking hot phonons.

Strandberg[36] has shown that the hot-phonon theory should lead to a different relation between saturation level and incident power. We have found that the steady-state saturation curve of the Cr^{+++} resonance in MgO follows the theoretical curve $(1+\gamma^2 H_{rf}^2 T_1 T_2^*)^{-1}$ with constant $T_1 T_2^*$ very well to over 90% saturation. The saturation curves of Fig. 8 point to the same conclusion. The bottleneck for energy transfer in dilute paramagnetic substances is between the spins and the lattice.

In more recent experiments with dilute gadolinium ethylsulphate and chrome alum, Davis, Strandberg, and Kyhl[37] have measured the true spin-lattice relaxation time. The interpretation of the data in this paper is in general agreement with the present conclusions, with the exception of the interpretation of Fig. 4. It was found that the recovery (relaxation) rate of the microwave susceptibility increased rapidly above a certain critical level of monitor power. This should not be ascribed to phonon heating at high monitor power levels, but is probably a consequence of the conventional rate equations. The recovery rate is $(1/T_1)+\gamma^2 H_{mon}^2 \times g(\nu)$. The measured relaxation is consequently $T_1(1+cH_{mon}^2)^{-1}$, where c is a constant.

Although it has been shown that phonon heating is neither a necessary nor a sufficient condition for the explanation of relaxation effects in the dilute paramagnetic substances studied, it may well exist on a limited scale. Due to the spin-spin processes the warmed phonon region should be at least as wide as the region of homogeneous spin saturation. Note that the phonon bandwidth is now a consequence rather than a cause of the homogeneous saturation. Suppose a paramagnetic resonance at 3000 Mc/sec in $K_3(0.995$ Co)(0.005 Cr)(CN)$_6$ has a spin-lattice relaxation time $T_1=10^{-2}$ sec and is saturated over an effective bandwidth of 60 Mc/sec. Suppose further that Raman processes are excluded. Let ΔT be the temperature difference between the phonons in the interior of the crystal with linear dimension $a=0.4$ cm; $c=1.5\times10^5$ cm/sec is the velocity of sound, and η is the heat transfer coefficient at the surface. Equate the power absorbed by spins to the power carried away by the phonons:

$$\frac{1}{4}\left(\frac{h}{kT}\right)Nh\nu T_1^{-1}=\frac{12\pi\nu^2\Delta\nu}{c^3}\frac{2c}{a}\eta k\Delta T.$$

With $N=1.7\times10^{19}$ ions/cc, $\eta=1$ and $T=4°$K and $\nu=3\times10^9$ cps, one finds $\Delta T=0.3°$K. Although this temperature rise is rather small, it indicates that a significant rise in phonon temperature may well occur in concentrated paramagnetic salts, especially when T_1 is also short. The interesting relaxation phenomena found by van der Marel[24,38] in concentrated salts at low temperatures appear to indicate phonon heating.

Recent experiments by Bowers and Mims[29] in nickel fluosilicate show that the acoustical impedance mismatch at the surface measured by η is not important. It makes no difference whether the crystal is cooled by helium vapor or liquid. Perhaps the phonon scattering in real crystals with physical and chemical imperfections is stronger than present theories indicate. Heat conduction experiments by Dransfeld[39] appear to show that the scattering of microwave phonons by electronic spins is not the most important scattering mechanism. Much further work is needed to clear up the phonon aspect of the problem, but in dilute paramagnetic salts above 1°K the phonon heating problem plays a minor role.

10. CONCLUSION

The results obtained in this paper may be summarized as follows:

1. In most dilute paramagnetic substances, in particular in dilute $K_3Cr(CN)_6$, $Cu(NH_4)_2(SO_4)_2$·6 H_2O, and $NiSiF_6$·6 H_2O, phonon heating plays a secondary role, if any, in the relaxation mechanism.

2. High-order spin-spin interactions, such as multiple simultaneous flip-flops, account for observed cross-saturation and cross-maser effects.

3. These processes determine a "cross-relaxation" time T_{21} which is intermediate between T_1 and T_2.

4. This time T_{21} determines how fast two nearby resonances or two spin systems are brought to the same effective temperature.

5. This time also determines the intermediate-frequency temperature-independent relaxation found by de Vryer and Gorter.

6. The existence and the extent of thermodynamic equilibrium in a multilevel spin system are characterized by a large number of cross-relaxation times.

7. Even so-called inhomogeneously broadened lines will usually show a homogeneous steady-state saturation, unless the inhomogeneity has a macroscopic spatial distribution.

8. Paramagnetic salts used in multiple-level masers are emissive over the full width of the magnetic resonance.

[35] Strandberg, Davis, Faughnan, Kyhl, and Wolga, Phys. Rev. 109, 1988 (1958).
[36] M. W. P. Strandberg, Phys. Rev. 110, 65 (1958).
[37] Davis, Strandberg, and Kyhl, Phys. Rev. 111, 1268 (1958).

[38] Van der Marel, van den Broek, and Gorter, Physica 24, 101 (1958).
[39] K. Dransfeld, Bull. Am. Phys. Soc. Ser. II, 3, 325 (1958).

9. The low-frequency limit of such masers is determined by the overlap of adjacent resonances.

Lattice Specific Heats near 0°K with an Application to Germanium*

PAUL M. MARCUS AND ANTHONY J. KENNEDY
Carnegie Institute of Technology, Pittsburgh, Pennsylvania
(Received November 17, 1958)

Formulas for the low-temperature lattice specific heat are developed on the basis of the general adiabatic and harmonic assumptions, independently of special models or numerical procedures. Explicit simple formulas are obtained for $\theta_D(0)$, the equivalent Debye characteristic temperature at 0°K, and for the curvature of $\theta_D(T)$ at 0°K. Discussions are given of the resulting dependence of $\theta_D(0)$ on physical parameters and the significance of the formula for $\theta_D(0)$ as a check on the basic assumptions, of the absence of a linear term in $\theta_D(T)$, and of the dependence of the curvature on the dispersion of elastic waves. $\theta_D(0)$ is calculated for Ge as 374.0°K; an error of ±2°K is estimated as due to errors in the elastic constants whereas the computational error is negligible. $\theta_D(T)$ is calculated for Ge for $[T/\theta_D(0)]<0.11$ using two models. The first is a simple model of the frequency spectrum which gives results like typical force-constant models, and disagrees with measurement. The second is a model of the frequency spectrum based on the direct measurements by inelastic neutron scattering; this model shows much greater dispersion, and gives much better agreement of $\theta_D(T)$ with measurement.

I. INTRODUCTION AND SUMMARY

THE technique of low-temperature specific heat measurements now provides sufficient accuracy at temperatures low enough to permit reasonable extrapolation to 0°K in many cases. Accordingly, attention may be focused on the limiting behavior at 0°K, which is a point of particular simplicity for theoretical discussion, as will be shown below. The observed specific heat curves show substantial deviations from the Debye approximation rather close to 0°K, even for simple monatomic lattices. Considerable work has been devoted to explaining these deviations as properties of various microscopic models of the dynamics of crystal lattices, and conversely, successful explanations support the validity of these models and the assumptions underlying them.[1] Several workers have paid particular attention to the limiting behavior at 0°K. Blackman[1] has emphasized the occurrence of deviations from the limiting T^3 law at substantially lower temperatures than the Debye approximation would give, on the basis of calculations on various force constant models. Bhatia and Horton[2] discuss the limiting curvature of the equivalent Debye charac-

teristic temperature, $\theta_D(T)$, at 0°K, and point out that $\theta_D(T)$ could curve upward although it usually curves downward.

Barron and Morrison[3] emphasize the importance of fitting specific heat data near 0°K, not only with terms in T^3 but also T^5 and T^7. Bhatia and Tauber, and Betts, Bhatia, and Wyman[4] have developed approximate methods for evaluating the limiting value of $\theta_D(T)$ at 0°K based on expansions in harmonic polynomials. (Older methods may be found in Blackman.[1]) Horton and Schiff[5] have applied similar approximate methods (refined somewhat) to the evaluation of the curvature of $\theta_D(T)$ at 0°K, and confirmed an upward curvature for a particular model of Pb. De Launay[6] has tabulated accurate values of $\theta_D(0)$ for cubic lattices over a range of elastic parameters and has also tabulated the curvature for a special force-constant model.

Most of the discussions of the low-temperature form of C_v or $\theta_D(T)$ in the above references, are complicated by the use of special force-constant models, or by special computational approximations, such as Houston's method.[2] In this paper we develop general expressions

[1] For recent reviews with many illustrations of specific heat behavior see, for example, M. Blackman, in *Handbuch der Physik* (Springer-Verlag, Berlin, 1955), Vol. VII, Part I, p. 325; D. H. Parkinson, in *Reports on Progress in Physics* (The Physical Society, London, 1958), Vol. XXI, p. 226.
[2] A. B. Bhatia and G. K. Horton, Phys. Rev. 98, 1715 (1955).
[3] T. H. K. Barron and J. A. Morrison, Can. J. Phys. 35, 799 (1957).
[4] A. B. Bhatia and G. E. Tauber, Phil. Mag. 45, 1211 (1954); Betts, Bhatia, and Wyman, Phys. Rev. 104, 37 (1956).
[5] G. K. Horton and H. Schiff, Can. J. Phys. 36, 1127 (1958).
[6] J. de Launay, in *Solid State Physics*, edited by F. Seitz and D. Turnbull (Academic Press, Inc., New York, 1956), Vol. 2, p. 219.